Research Article

The Journal of Computational Multiphase Flows

The Journal of Computational Multiphase Flows
2017, Vol. 9(1) 47–53

DOI: 10.1177/1757482X16688476
journals.sagepub.com/home/cmf
SAGE

Numerical analysis of an annular water–air jet pump with self-induced oscillation mixing chamber

Xiaogang Deng[1], Jingliang Dong[2], Zhentao Wang[3] and Jiyuan Tu[4]

Abstract

This paper presents an improved annular water–air jet pump concept design through integrating a self-induced oscillation mixing chamber with the conventional annular jet pump (AJP). The internal flow characteristics for both conventional and improved AJP were numerically investigated and compared by a validated computational fluid dynamics model. The numerical comparison demonstrated an approximately 10% pumping performance increase compared with the conventional pump, which is mostly attributed to the improved mass and energy transfer along the oscillating phase interface. Furthermore, transient flow analysis was conducted to resolve the unsteady self-introduced oscillation. The results revealed the self-introduced oscillation induces a continuous break-up and formation of fresh water–air interfaces, which exhibits a periodic feature with a dominant frequency of 147 Hz for the current design under given operational conditions. This study contributes toward a better understanding of the internal annular water–air jet pump flow patterns, and also demonstrates the feasibility of incorporating self-introduced oscillation chamber into AJP design.

Keywords

Annular jet pump, self-induced oscillation, numerical simulation, water–air interface, dominant frequency

Date received: 7 July 2016; accepted: 3 November 2016

Introduction

Jet pumps are widely used to create and maintain a vacuum operating environment in chemistry, petroleum, metallurgy, refrigeration and other industries. Compared with rotary pump, jet pump has various superior advantages such as simplicity and reliability, low capital cost for installation and maintenance, and capability of handling high operating temperature.[1] The main components of a jet pump consist of an active (primary) nozzle, a passive (suction) nozzle, a throat tube (also referred to as the mixing tube) and a diffuser on the downstream. The absence of moving mechanical parts eliminates the potential operational problems associated with bearing, sealing and lubrication.[2]

There are two types of jet pumps based on different primary and secondary fluid input arrangements.[3] The first type is the central jet pump (CJP), which applies the primary fluid to the inner nozzle and connects the annular periphery surrounding nozzle with the secondary fluid. The second one is the annular jet pump (AJP), in which the suction fluid passes through the inner nozzle and the primary fluid is connected with the annular nozzle on the periphery of the suction tube.

For CJPs, it has been studied intensively for decades focusing on geometrical design[4–8] and operational parameters.[1,9,10] On the other hand, the research of AJPs remains relatively unfolded. Shimizu et al.[11] experimentally investigated the relation between configuration

[1]Chongqing University of Science and Technology Shapingba District Chongqing, Chongqing 401331 China
[2]Chongqing University Chongqing, China
[3]Jiangsu University, Jiangsu, China
[4]RMIT University, Bundoora, Victoria, Australia

Corresponding author:
Jiyuan Tu, RMIT University, Plenty Road, Bundoora, Victoria 3083, Australia.
Email: jiyuan.tu@rmit.edu.au

and performance of the AJPs and compared it with that of the CJPs. Twenty-five different kinds of pumps were used in the experiments, and a maximum efficiency of 36% was reached. Kim et al.[12] studied the hydrodynamic characteristics of a horizontal annular type water–air AJP both numerically and experimentally. Their flow visualization reveals that water/air mixed flow is immediately generated at the throat region, and the buoyant effect is partially observed at low water flow rate. Lyu et al.[13] conducted a structure optimization study of AJPs through the design of experiments (DoE) and computational fluid dynamics (CFD) methods. The results showed that two-factor's reciprocal action is more applicable than that of single factor on the AJP's performance.

Despite extensive research studies that have been conducted, how to continue improve the jet pumping performance of the conventional AJPs, especially for the further improvement of fluids mixing remains challenging. Li et al.[14] numerically modelled the self-induced oscillations in the mixing head of a reaction injection moulding machine, which provides a starting point towards the understanding of the quantities of the oscillatory flow. Wang et al.[15] applied the self-induced oscillation into the development of the pulsed jet drilling technology for the exploration and production of oil fields. Their results show a negative pressure (vacuum) zone is formed in the oscillation cavity, which ensures the suction of enough annular fluids and benefits the formation of an efficient pulsed jet. However, to the best of the authors' knowledge, no relevant research studies have applied the concept of self-induced oscillation into the current AJP geometrical design. Thus, in this study, an improved pump design through integrating a self-induced oscillation mixing chamber with the existing AJP design was proposed, and the internal flow characteristics and overall pumping performance were numerically investigated.

Method

Geometrical and operational parameters

A schematic diagram illustrating both conventional and improved AJP designs is shown in Figure 1, where water is used as the motive fluid and connected with the annular nozzle on the periphery of the inner suction tube, while the air is used as the entrained fluid and connected with the inner nozzle. The conventional AJP geometrical parameters were referred from Park and Yang.[16] As mentioned earlier, the main difference between the conventional AJP and the improved AJP design is the self-induced oscillation chamber, which is an enlarged cylindrical cavity with a cone-shaped impinge downstream sidewall, and its geometrical

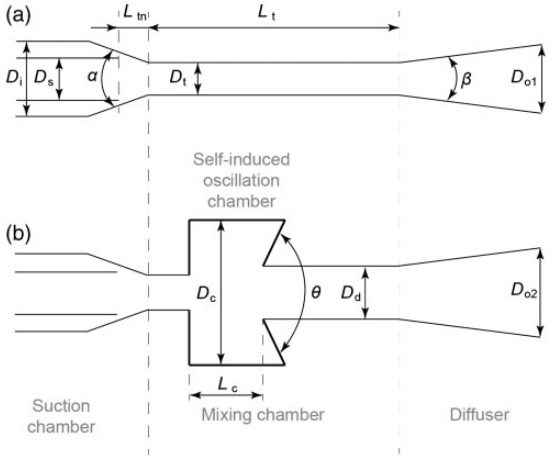

Figure 1. Schematic diagrams of annular jet pump: (a) the conventional design and (b) the improved design with self-induced oscillation chamber.

Table 1. Geometric dimensions of the studied AJPs.

Dimension	D_i	D_s	D_t	D_c	D_d	D_{o1}	D_{o2}	Lt	α	β	θ
Value (mm)	50	26	26	140	36	45	35	290	59°	4°	120°

AJP: annular jet pump.

configuration was referred from Liao et al.[17] All basic pump parameters are listed in Table 1.

CFD modelling strategy

In the present study, the commercial CFD code ANSYS–Fluent was employed as the research platform. Both conventional and improved AJPs were assumed into 2D axisymmetric domains.[1] Both conventional and improved AJP CAD models were meshed into quadrilateral structural elements, and mesh refinements were applied at the vicinity of gas–liquid interface.

For multiphase flow modelling, there are two commonly used approaches: the Euler–Lagrangian approach or the Euler–Euler approach. Kim et al.[12] suggested to choose the Eulerian multiphase model to simulate the water–air multiphase flow in AJPs as dispersed-phase volume fractions of bubbly flow normally exceeds 10%. Therefore, the present work adopts the Euler–Euler method, where the different phases are treated as interpenetrating continua and the conservation equations for all phases are similar. The governing equations are as follows:

Continuity equation for phase i is

$$\frac{\partial}{\partial t}(\alpha_i \rho_i) + \nabla \cdot \left(\alpha_i \rho_i \vec{v}_i\right) = 0$$

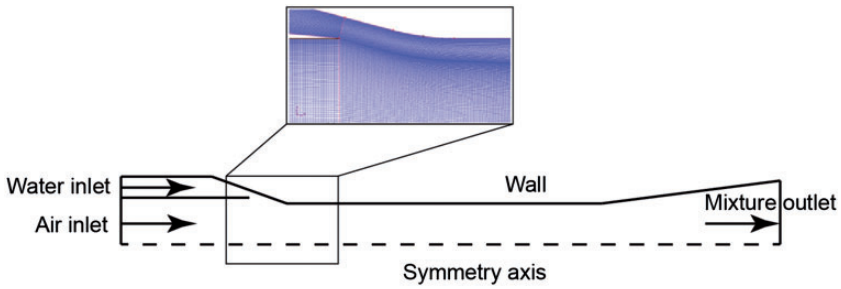

Figure 2. Numerical boundary conditions and regional mesh refinement.

Momentum equation for the air phase yields

$$\frac{\partial}{\partial t}\left(\alpha_g \rho_g \vec{v}_g\right) + \nabla \cdot \left(\alpha_g \rho_g \vec{v}_g \vec{v}_g\right) = -\alpha_g \nabla p + \nabla \cdot \bar{\tau}_g + \alpha_g \rho_g \vec{g} + \vec{R}_{gl} + \left(\vec{F}_g + \vec{F}_{lift,g} + \vec{F}_{td,g}\right)$$

where $\bar{\tau}_g$ is the gas phase stress–stain tensor given as

$$\bar{\tau}_g = \alpha_g \mu_g \left(\nabla \vec{v}_g + \nabla \vec{v}_g^T\right) + \alpha_g \left(\lambda_g - \frac{2}{3}\mu_g\right) \nabla \cdot \vec{v}_g \bar{I}$$

The flow inside the pump was assumed to be steady and incompressible flow, controlled by the Reynolds averaging Navier–Stokes equations and the continuity equation. In this study, three widely-used k–ε turbulence model variations (the standard, realizable and RNG model) were selected to resolve the turbulence characteristics with the standard wall function adopted to resolve the near-wall region. Velocity boundary conditions were applied on the inlets boundaries and pressure boundary condition on the outlet boundary. The governing equations were discredited by the finite volume method and the secondary upwind scheme was adopted for spatial discretization of the convection terms. The SIMPLE algorithm was employed to solve the coupling the pressure and velocity.

Prior to performing the simulations, a mesh independence study was conducted to eliminate the influence of the numerical element size. The grid number was initially made at about 72,000 and later increased to about 421,000 to confirm that the results were grid independent. The air entrainment value was selected as grid evaluation target for all mesh configurations, and detailed numerical results are listed in Table 2. As the air entrainment predictions between the medium and fine meshes were very close, the medium mesh scale was selected for further numerical simulations.

Table 2. Mesh independence study.

	Elements number		Air entrainment (L/s)
AJP	Low	72,500	0.99
	Medium	234,000	1.06
	High	421,000	1.07
Improved AJP	Low	74,000	1.04
	Medium	275,100	1.1
	High	433,000	1.105

AJP: annular jet pump.

Table 3. Tube tip position along with its corresponding operating conditions.

Pitch	1	2	3	4	5	6	7	8	9	10
L_{tn} (mm)	2.5	4	5.5	7	8.5	10	11.5	13	14.5	16
A_{tn} (mm^2)	56	91	126	163	200	238	276	316	357	398
Q_p (m^3/h)	3.0	5.6	9.4	12.5	14.5	15.5	16.4	16.8	17.0	17.5

Results and discussions

Validation of CFD simulation

To validate the accuracy of the proposed numerical modelling approach, the experimental work conducted by Park and Yang[16] was used as validation target. This referred experimental study investigated the influences of both operational parameters and geometrical parameters on overall pumping performance. In the present study, only the relevant experimental data considering the variation of geometrical parameters was selected for results comparison. In detail, the tip position (L_{tn}) indicating the distance between the annular nozzle exit plane and the inlet of the parallel mixing tube was adjusted, and 10 positions with an interval of 1.5 mm were studied. All tube tip positions (L_{tn}) along with its corresponding operating primary fluid conditions (Q_p) are listed in Table 3.

Figure 3 compares the numerical simulation results with the referred experimental data based on the conventional AJP design by changing the suction tube exit tip position (L_{tn}). In general, the numerical predictions agree well with the experimental data, the air entrainment flow rate first increases with the increase of L_{tn} and peaks at 35 m^3/h when $L_{tn} = 5.5$ mm. While with

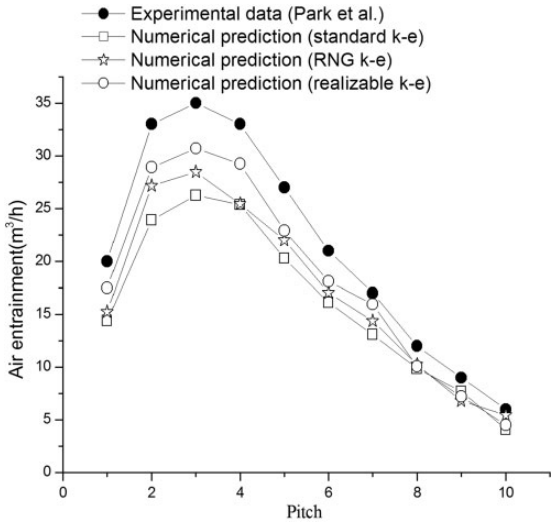

Figure 3. Numerical results comparison with the referred experimental study.

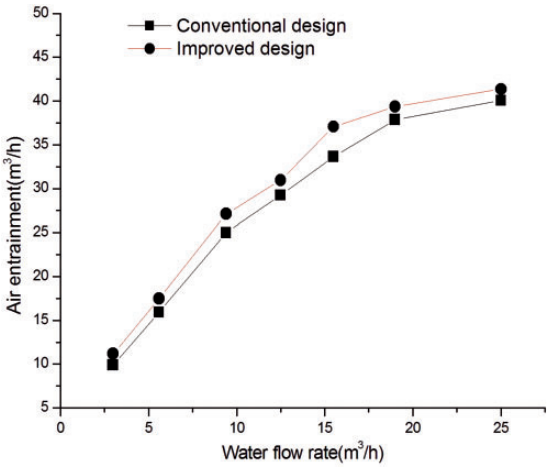

Figure 4. Numerical comparison of pumping performance between the conventional and the improved AJPs.

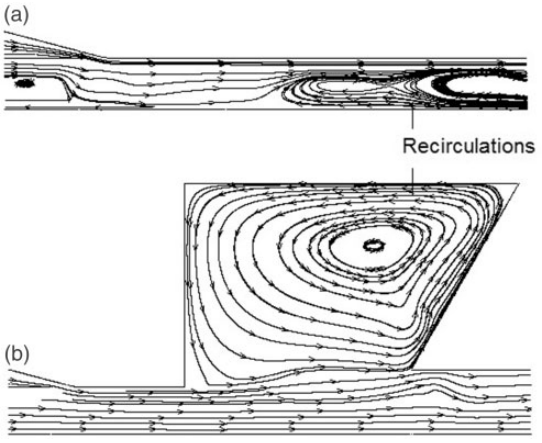

Figure 5. Streamlines comparison between (a) the conventional and (b) the improved AJPs.

the further L_{tn} increase, the entrained air flow rate decreases rapidly, and reaches the lowest value of $6\,m^3/h$ when $L_{tn} = 16\,mm$.

As the internal flow regime is turbulence, the turbulence flow predicting is largely relying on the chosen of the suitable turbulence model. In the present study, three widely used turbulent models were assessed. It was demonstrated that the realizable k–ε turbulence model provides the closest entrainment performance prediction compared with the experimental data. However, the numerical simulation slightly underpredicted the pumping performance, especially for the prediction of the peak value when $L_{tn} = 5.5\,mm$, with a discrepancy of 14%.

Despite the existence of the numerical prediction discrepancy compared with experimental data, the validity of the proposed numerical modelling approach was verified, and all further simulations were solved by the same solver configurations using the realizable k–ε turbulence model.

Comparison between the conventional and improved AJPs

Figure 4 compares the pumping performance of the conventional and improved AJPs in terms of the entrained air flow rate on the basis of a fixed tip position ($L_{tn} = 5.5\,mm$). It was found that both designs exhibit similar air entrainment profile trend, which indicates a positive correlation between the air entrainment flow rate and the motive water flow rate. However, the improved AJP with the self-induced oscillation chamber showed a superior air entrainment performance for all considered motive water flow rates compared with the conventional AJP, and the maximum pumping improvement percentage (approximately 12%) occurs at the water flow rate of $15\,m^3/h$.

To provide a better understanding of the internal flow patterns of the studies, AJPs, the streamlines, phase fraction distribution and the turbulence kinetic energy of the gas phase based on the case with maximum performance improvement as mentioned earlier were selected for flow pattern analysis.

Figure 5 compares the streamlines between the conventional and improved AJP. For the conventional AJP, a significant flow recirculation which occupies more than half of the throat was found downstream of the mixing tube. In comparison, after integrating the self-induced oscillation chamber with the mixing tube, this flow recirculation vanished and the flow interaction between the gas phase (air) and liquid phase (water) was enhanced with the formation of a counter-clockwise vortex.

Figures 6 and 7 provide a detailed phase distribution and turbulence flow characteristics comparison. For the conventional AJP (Figure 6(a)), a clear air–water phase interface was established, indicating the interaction between the motive water and the entrained air is mainly relying on the viscous fraction along the phase interface region. On the contrary, the improved AJP with self-induce oscillation chamber showed a different phase mixing pattern (Figure 6(b)). Due to the abrupt cross-sectional area expansion, the air–water phase interface was disrupted into discontinuous fragments, and a better phase mixing was reached in the self-induced oscillation chamber. Figure 7 illustrates the momentum exchange between these two phases for both AJPs. For the conventional AJP, the high turbulence kinetic energy for the entrained air occurs along the phase interface. Therefore, the momentum

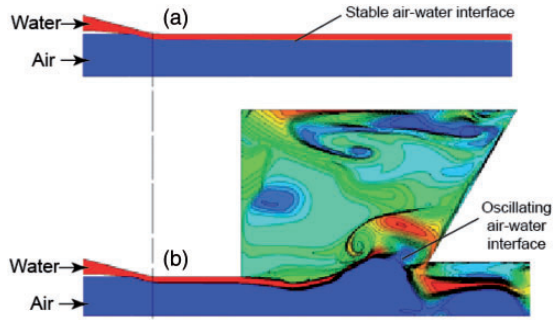

Figure 6. Phase volume fraction comparison between (a) the conventional and (b) the improved AJPs.

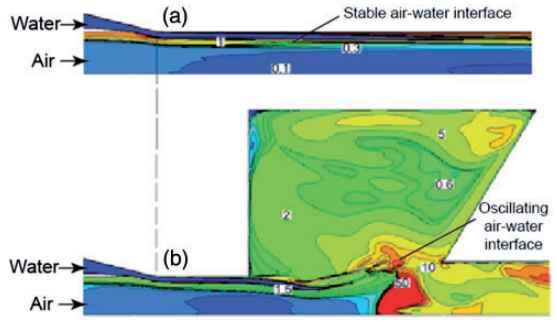

Figure 7. Turbulence kinetic energy comparison between (a) the conventional and (b) the improved AJPs.

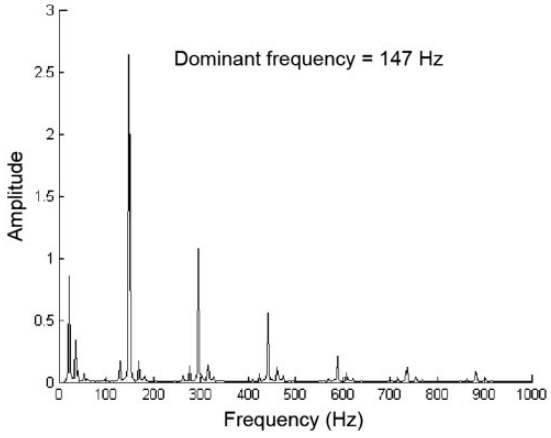

Figure 9. Time domain analysis of the transient air flow rate profile.

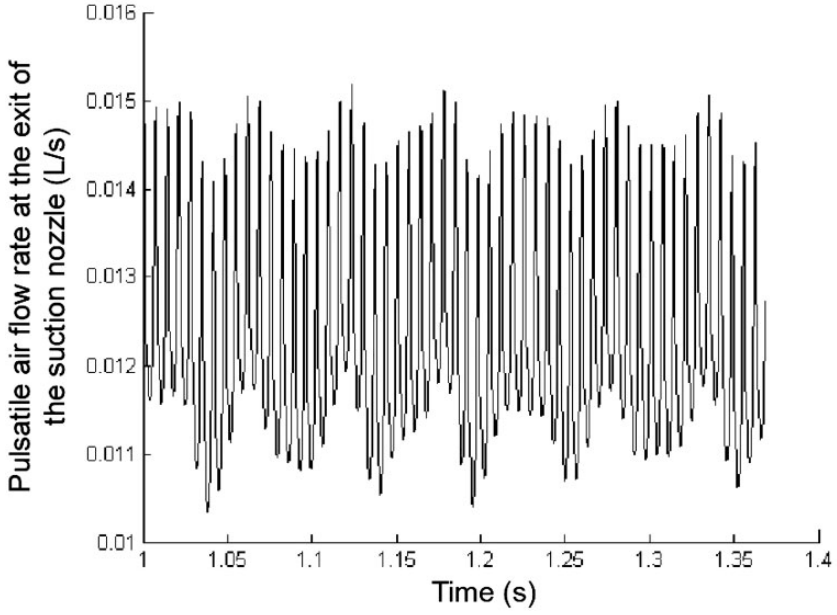

Figure 8. The pulsatile entrained air flow rate variation over time.

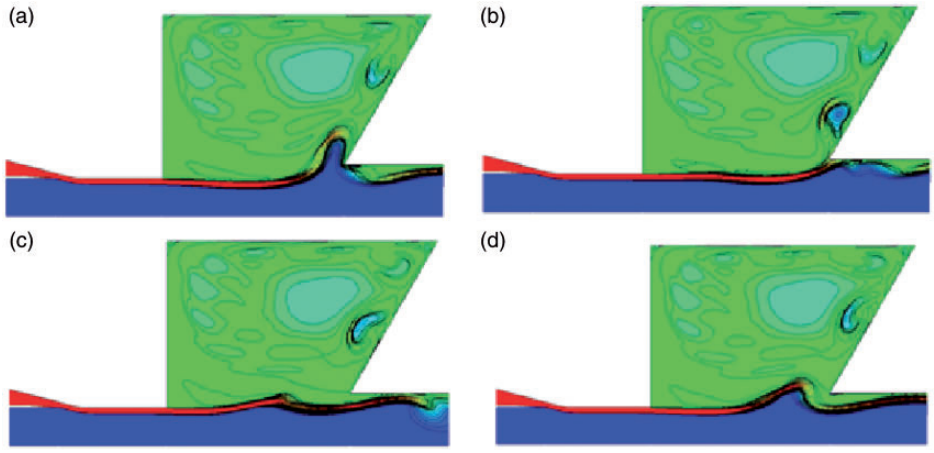

Figure 10. Four typical events representing the transient phase volume fraction variation over one cycle.

exchange mainly occurs along the limited region of the phase interface, which implies the energy transfer from the motive fluid to the entrained fluid is not sufficient. While for the improved AJP, larger proportion of gas phase (air) with high turbulence kinetic energy was found both in the self-induce oscillation chamber and the following downstream mixing tube. This demonstrates the self-induce oscillation chamber can considerably enhance the phase mixing and energy exchanger, which ultimately improve the AJP pumping performance.

Unsteady flow patterns in the improved AJP

As the energy exchange between water and air phases is highly unsteady with fluctuations, time domain analysis based on a transient flow simulation was performed to better illustrate this dynamic energy exchanging process.

Through monitoring the unsteady air volume flow rate at the outlet of the jet pump, it was found that the air volume flow rate profile shows a periodic pattern over time with its flow rate ranges between 0.01 L/s and 0.015 L/s (Figure 8), while the frequency of the volume flow rate variation remains relatively stable. To reveal this variation frequency, a Laplace transform was carried out based on the current profile, and its domain frequency was found to be 147 Hz (Figure 9). Therefore, a typical period of the energy exchanging process takes approximately 0.0068 s for the improved AJP with the given operation conditions.

Figure 10 presents the phase variation of water and air over a single cycle. At the beginning phase (Figure 10(a)), a raised "air bubble" starts to protrude towards the self-induced oscillation chamber at the sloped downstream chamber edge. After that, as shown in Figure 10(b), the "air bubble" breaks away from the air–water interface, and flows into the self-induced oscillation chamber along with the counter-clockwise vortex (Figure 5(b)). Then the "air bubble" dissipates into the chamber space, where both water and air are almost sufficiently mixed (Figure 10(c)). Finally, the whole period repeats again as demonstrated in Figure 10(d), in which similar air–water interface oscillation pattern with that shown in Figure 10(a) was formed.

Conclusions

This paper presents an improved AJP concept design through integrating a self-introduced oscillation chamber with the conventional AJP design. The numerical comparison between the conventional and the improved AJPs demonstrated a considerable performance improvement (approximately 10%) compared with the conventional AJP. The phase volume fraction and turbulence kinetic energy analysis revealed the air–water interface dominates the energy transfer between the primary and the secondary fluids. For the conventional design, the phase interface remains relatively stable with a clearly formed boundary between those phases. However, for the improved design, the phase interface shows an oscillating pattern, where more secondary fluid (air in present study) can be entrained and dispersed into the primary fluid (water in this paper) due to the continuous formation of fresh phase interfaces.

In the present study, numerical simulations based on simplified 2D fluid assumption were conducted, while this assumption remains to be further improved in the further study. Additionally, more experimental efforts such as flow imaging are needed to reveal the complex internal flow and mixing patterns. Despite these limitations, this study demonstrates the performance improvement through integrating the self-introduced oscillation chamber with the current conventional AJP design. The research findings can contribute an

improved concept AJP design for future practical applications.

Declaration of conflicting interests

The author(s) declared no potential conflict of interest with respect to the research, authorship, and/or publication of this article.

Funding

The author(s) disclosed receipt of the following financial support for the research, authorship, and/or publication of this article: This research is financially supported by the National Natural Science Foundation of China (Contract ID: 51376204), the Fundamental Research Funds for the Central Universities (Project ID: 106112016CDJCR211221) and the Foundation and Advanced Technology Research Project in Chongqing (Contract ID: cstc2014jcyjA90003).

References

1. Wang X and Dong J. Numerical study on the performances of steam-jet vacuum pump at different operating conditions. *Vacuum* 2010; 84: 1341–1346.
2. Dong J, Wang X and Tu JY. Numerical research about the internal flow of steam-jet vacuum pump: evaluation of turbulence models and determination of the shock-mixing layer. *Phys Proc* 2012; 32: 614–622.
3. Wang D. *Analysis and design of air-jet pumps for pneumatic transportation of bulk solids in pipelines*. PhD Thesis, University of Wollongong, Australia.
4. Chellappan S and Ramaiyan G. Experimental study of design parameters of gas/solid injector feeder. *Powder Technol* 1986; 48: 141–144.
5. Croft DR and Lilley DG. Jet pump design and performance analysis. In: *14th Aerospace Sciences Meeting*, Washington, DC, U.S.A. doi: 10.2514/6.1976-183.
6. Hatzlavramldls DT. Modelling and design of jet pumps. *SPE Prod Eng* 1991; 6: 413–419.
7. Neve RS. Diffuser performance in two-phase jet pumps. *Int J Multiph Flow* 1991; 17: 267–272.
8. Senthil Kumar R, Kumaraswamy S and Mani A. Experimental investigations on a two-phase jet pump used in desalination systems. *Desalination* 2007; 204: 437–447.
9. Aldas K and Yapici R. Investigation of effects of scale and surface roughness on efficiency of water jet pumps using CFD. *Eng Appl Comput Fluid Mech* 2014; 8: 14–25.
10. Meakhail T and Teaima I. Experimental and numerical studies of the effect of area ratio and driving pressure on the performance of water and slurry jet pumps. *J Mech Eng Sci* 2011; 226: 2250–2266.
11. Shimizu Y, Nakamura S, Kuzuhara S, et al. Studies of the configuration and performance of annular type jet pumps. *J Fluid Eng* 1987; 109: 205–212.
12. Kim YK, Lee DY, Kim HD, et al. An experimental and numerical study on hydrodynamic characteristics of horizontal annular type water–air ejector. *J Mech Sci Technol* 2012; 26: 2773–2781.
13. Lyu Q, Xiao Z, Zeng Q, et al. Implementation of design of experiment for structural optimization of annular jet pumps. *J Mech Sci Technol* 2016; 30: 585–592.
14. Li X, Santos RJ and Lopes JCB. Modelling of self-induced oscillations in the mixing head of a RIM machine. *Can J Chem Eng* 2007; 85: 45–54.
15. Wang R, Du Y, Ni H, et al. Hydrodynamic analysis of suck-in pulsed jet in well drilling. *J Hydrodynam B* 2011; 23: 34–41.
16. Park S and Yang H. Flow and oxygen-transfer characteristics in an aeration system using an annular nozzle ejector. *Indust Eng Chem Res* 2013; 2013: 1756–1763.
17. Liao Z, Tang C and Wang G. A new type of nozzle for oil-well drill bits. Paper presented at the 10th international symposium on jet cutting technology, the Netherlands.